OFFICE OF NAVAL RESEARCH

Research Contract: N00014-90-J-1178
R&T Code: 413r008---01

Principal Investigator: **R. Stanley Williams**
Organization: **Regents of the University of California**

TECHNICAL REPORT No. 19

EVIDENCE FOR THE DEPENDENCE OF THE SPUTTER YIELD OF GRAPHITE ON ION BOMBARDMENT FLUENCE

by

E.J. Snyder, D.A. Baugh, R.S. Williams, E.A. Eklund and M.S. Anderson

Prepared for publication in

Surface Science

University of California, Los Angeles
Department of Chemistry & Biochemistry and Solid State Sciences Center
Los Angeles, CA 90024-1569

REPORT DOCUMENTATION PAGE

Form Approved
OMB No 0704-0188

1. AGENCY USE ONLY (Leave blank)	2. REPORT DATE	3. REPORT TYPE AND DATES COVERED
		Technical 6/1/91-5/31/92

4. TITLE AND SUBTITLE
EVIDENCE FOR THE DEPENDENCE OF THE SPUTTER YIELD OF GRAPHITE ON ION BOMBARDMENT FLUENCE

5. FUNDING NUMBERS
N00014-90-J-1178

6. AUTHOR(S)
E.J. Snyder, D.A. Baugh, R.S. Williams, E.A. Eklund, M.S. Anderson

7. PERFORMING ORGANIZATION NAME(S) AND ADDRESS(ES)
Regents of the University of California
University of California
405 Hilgard Ave.
Los Angeles, CA 90024

8. PERFORMING ORGANIZATION REPORT NUMBER
Technical Report # 19

9. SPONSORING/MONITORING AGENCY NAME(S) AND ADDRESS(ES)
Office of Naval Research
Chemistry Program
800 N. Quincy Street
Arlington, VA 22217-5000

10. SPONSORING/MONITORING AGENCY REPORT NUMBER

11. SUPPLEMENTARY NOTES
Prepared for publication in " Surface Science"

12a. DISTRIBUTION AVAILABILITY STATEMENT
Approved for public release.
Distribution unlimited.

12b. DISTRIBUTION CODE

13. ABSTRACT (Maximum 200 words)

The scanning tunneling microscope (STM) and the atomic force microscope (AFM) were both used to study the evolution of the morphology of graphite (0001) surfaces etched with 5 keV Ar^+ ions as a function of both ion beam flux and fluence. STM and AFM topographs collected after ion beam exposure show surface features that increase in average size as a function of ion beam fluence, but which have a non-monotonic dependence on ion beam flux. Furthermore, the surface roughness does not follow a square root dependence with respect to the ion fluence, as expected for a stochastic process. One explanation for this behavior is that the sputter yield for graphite is a function of the ion beam fluence.

14. SUBJECT TERMS	15. NUMBER OF PAGES
	16 pages
	16. PRICE CODE

17. SECURITY CLASSIFICATION OF REPORT	18. SECURITY CLASSIFICATION OF THIS PAGE	19. SECURITY CLASSIFICATION OF ABSTRACT	20. LIMITATION OF ABSTRACT
Unclassified	Unclassified	Unclassified	UL

Evidence for the Dependence of the Sputter Yield of Graphite on Ion Bombardment Fluence

ERIC J. SNYDER*, DELROY A. BAUGH*, R. STANLEY WILLIAMS*, ELLIOTT A. EKLUND**, AND MARK S. ANDERSON***

*Department of Chemistry and Biochemistry and Solid State Science Center, University of California Los Angeles, Los Angeles, CA 90024-1569
** IBM Research Division, Yorktown Heights, NY 10598
*** Jet Propulsion Laboratories, Pasadena, CA 91109-8099

ABSTRACT

The scanning tunneling microscope (STM) and the atomic force microscope (AFM) were both used to study the evolution of the morphology of graphite (0001) surfaces etched with 5 keV Ar^+ ions as a function of both ion beam flux and fluence. STM and AFM topographs collected after ion beam exposure show surface features that increase in average size as a function of ion beam fluence, but which have a non-monotonic dependence on ion beam flux. Furthermore, the surface roughness does not follow a square root dependence with respect to the ion fluence, as expected for a stochastic process. One explanation for this behavior is that the sputter yield for graphite is a function of the ion beam fluence.

Ion beam etching (IBE) is a widely used technique for surface preparation and analysis.[1] Nonequillibrium surfaces produced by this technique have topographies that are known to depend on the sputtering conditions.[2] A complete, fundamental understanding of the interaction of surfaces with ion beam radiation, however, is not yet available to the materials scientist or process engineer.[3]

Surfaces are roughened, not smoothened, by IBE at the sub-micron level. The influence of the stochastic nature of sputter deposition has been modeled by Karunsari, Bruinsma, and Rudnick[4] by including a shot noise term in a linear response theory. This model has recently been modified for IBE by changing the sign of the derivative of the surface height with respect to time, and was found to qualitatively agree with experimental data.[5] In particular, the surface roughness was found to depend on the sample temperature, the ion fluence, and the ion flux during IBE.

The poresent paper is a continuation of our prior work utilizing scanning tunneling microscopy (STM) to study the surface morphology of ion-etched graphite surfaces.[5,6] In addition to STM, atomic force microscopy (AFM) and Fourier transform infrared (FTIR) spectroscopy were also used to characterize the ion- etched surfaces in this work. The STM and AFM were used because these two instruments directly produce quantitative surface topography data, in contrast to scanning electron microscope and optical characterizations. The height autocovariance function for these ion-etched surfaces was then computed from the STM and AFM numerical data and compared to model predictions.

The graphite (0001) surfaces studied in these experiments were prepared by cleaving highly oriented pyrolytic graphite (HOPG) samples; these surfaces were atomically flat over tens of thousands of square angstroms[7] prior to ion beam

exposure. Graphite is also inert in air and has a very rigid lattice, as demonstrated by its high melting temperature of approximately 3800°C. This means that diffusion after ion beam exposure is limited; the etching features are 'frozen in' to the surface and can be scanned with the STM or AFM long after the ion beam exposure.

After cleaving, the samples were scanned with STM (described elsewhere[5]) to insure that they were atomically flat and then placed in an ultrahigh vacuum chamber and pumped down to about 10^{-9} torr. They were then exposed to Ar^+ ions accelerated through a potential of 5 keV and rastered over a 9 mm^2 area of the graphite surface at an angle about 45° off the surface normal. A small positive bias (45 volts) was applied to the sample to suppress secondary electron emission. In these experiments, the total ion fluence at the center of the sample was 10^{19} ions/cm^2 and the ion flux conditions were 6.9 x 10^{13}, 3.5 x 10^{14}, and 6.9 x 10^{14} ions/cm^2/sec.

After sputtering, the samples were removed from the UHV system through a nitrogen filled glovebox and stored there when they were not being scanned in the STM or AFM. STM scans were collected in a range of sizes from 250Å x 250 Å up to 2400Å x 2400A; AFM scans were collected at sizes from 5000Å x 5000Å up to 100,000Å x 100,000A. The STM was operated in the constant current or topographic mode at a tunnel current of 0.5 nA, sample to tip bias of -100 mV, and in air at room temperature. The AFM used was a Digital Instruments Nanoscope II also operated in ambient air. Since oxidation of exposed ion etched graphite surfaces has been observed in samples exposed to ambient air for several days,[5] we compared the FTIR reflectance spectrum[8] (Analect FTIR model fXA-530) of an IBE sample freshly removed from vacuum to the same sample after 8 hours of exposure to ambient air. We did not observe any chemical changes at the surface, and since samples scanned with both STM and AFM were not exposed to ambient

air for more than 8 hours, contributions to surface morphology due to oxidation were neglected.

In prior STM studies of rough surfaces, topographs were collected that were shown to depend on the shape and sharpness of the tips used to collect the data.[9-12] In particular, surfaces with sharp protrusions can yield images of the sides of the tip, and blunt tips tend to produce images which appear smoother than they actually are because of the inability of the blunt tip to properly sample small, sharp features. We have been particularly careful to avoid tip artifacts in this study. In both instruments, topographs were collected with more than one tip and over several areas of the same sample. Furthermore, we did not filter or smoothen the data collected in this study prior to analysis. Most of the data collected was reproducible from sample to sample, even with different tips. Topographs with tip artifacts were observed but not analyzed for this study.

In these experiments, we varied the Ar^+ ion flux and compared the topography of the samples etched with 10^{19} ions/cm^2 to prior data at the same fluxes but at different fluences.[5] With the addition of the AFM, we were able to scan much larger areas of the sputtered surfaces. These extended range scans turned out to be crucial to properly identify and quantify the characteristic lengths and heights of the features produced with a fluence of 10^{19} ions/cm^2. Three large scale AFM topographs are shown in Fig. 1. The average feature heights are larger for the higher two fluxes, whereas the average feature to feature length on the surface increases going from the lowest to the intermediate flux and then decreases slightly at the highest flux. There is also a definite anisotropy in the average feature lengths in all three topographs in Fig. 1. This was verified to be consistent over large areas of the sample, and the longer features were parallel to the projection of the incident ion beam on the surface. This indicates that shadowing[4] played a role in the development of the surface features at the high

fluence used in this study. No significant anisotropy was observed at the lower fluences studied previously,[5] which indicates that the surface features must reach some critical height for a beam incidence angle of 45° before shadowing becomes important.

We calculated the autocovariance function from the topographic data as follows:

$$G(|\mathbf{r}_2 - \mathbf{r}_1|) = \langle h(\mathbf{r}_2)\, h(\mathbf{r}_1) \rangle - \langle h(\mathbf{r}) \rangle^2 , \qquad (1)$$

where $h(\mathbf{r}_i)$ is the height of the surface at position $\mathbf{r}_i$ and $L = |\mathbf{r}_2 - \mathbf{r}_1|$ is a separation length on the surface. This function provided a quantitative determination of the base to peak height variation and of the short range lateral correlation of the surface features. In particular, $\delta=[G(0)]^{1/2}$ is the interface width or standard deviation of heights on the surface. Also, if the initial drop off in the autocovariance function is approximated by a gaussian distribution, then the standard deviation of that gaussian is the characteristic feature separation length λ parallel to the surface (see Fig. 2). For the fluence of 10^{19} ions/cm^2, these λ values for the IBE surfaces were independent of whether they were obtained from the AFM or the STM topographic data.

Table 1 summarizes these values for the additional high fluence data reported here and for the prior data at lower fluences.[5] For the entire set of four fluences and three fluxes, the correlation lengths and interface widths clearly increase with increasing fluence for all the fluxes, which is not surprising. Since the surfaces in all of these experiments were initially atomically flat, the increase in the interface widths is somehow related to the amount of material removed during the sputtering process. A TRIM[13] Monte Carlo calculation predicted that on average 1.5 C atoms are removed from graphite for every incident Ar^+ ion

under these sputtering conditions. Therefore, a fluence of 10^{19} ions/cm^2 would correspond to the removal of about 4000 monolayers of graphite.

Figure 3 shows the dependence of the interface width as a function of ion fluence for all three fluxes; it is almost a first power relationship. This result is very surprising, because a stochastic model of ion etching predicts[5] that the interface width, δ, should scale as the square root of the amount of material removed, which is usually assumed to be directly proportional to the ion fluence:

$$\delta \approx d (Q Y/\rho)^{0.5} \qquad (2)$$

where d is the interlayer spacing for graphite, Y is the sputter yield, ρ is the area number density of a graphite plane, and Q is the ion beam fluence. Equation 2 is also plotted along with the experimental data in Fig. 3 for Y=1.5 (dashed line); it clearly diverges from the data at high fluences. Other surface effects such as diffusion and sputter redeposition are healing mechanisms; they tend to smoothen features on the surface and therefore could not be responsible for an increase in the interface width.[5]

One explanation for the data in Fig. 3 is that the sputter yield is actually a function of the ion fluence:

$$Y \approx Y_0 (1 + \beta Q) \qquad \text{and} \qquad (3)$$

$$\delta \approx d [Y_0 (1 + \beta Q) Q / \rho]^{0.5}, \qquad (4)$$

where β is a system-dependent parameter. Equation 4 is also plotted with the data in Fig. 3 (solid line). The two parameters Y_0 and β were best fit to the

experimental δ vs. Q data (ignoring the single data point for Q = 10^{16} ions/cm^2 and J = 7x10^{14} ions/cm^2/sec, which has been previously shown to be anomalous[5]); the values of Y_0 and β found in the fit shown in Fig. 3 are 1.25 atoms/ion and 2 x 10^{-18} cm^2/ion respectively. This best fit value of Y_0 is interesting because it agrees fairly well with the value of 1.5 independently calculated from the Monte Carlo simulation, which essentially models the sputter yield from a pristine surface.

The dependence of the sputter yield on fluence could physically correspond to chemical damage to the graphite surface. It is important to remember that the surface before IBE in all of these experiments was essentially a perfectly flat, regular graphite crystal layer. As the ions break up the rigid pi-orbital bond network in the surface layers, the damaged surface could become susceptible to enhanced sputter removal by other incoming ions. This effect by itself, however, would saturate at high enough fluences because the depth of damaged layers should tend to reach a steady state value. However at a fluence of 10^{19} ions/cm^2, which corresponds to an average of about 2500 Ar^+ ions per surface carbon atom, we see no drop off in the dependence of the interface width towards a square root dependence. If Eq. 4 is valid, then the sputter yield of a surface exposed to a fluence of 10^{19} ions/cm^2 would be about 26 ejected carbon atoms per incident Ar^+ ion from the fit shown in Fig. 3, which is very high compared to Y_0. This suggests that clusters may be ejected from heavily bombarded surfaces, and that the total amount of material removed by the 10^{19} ions/cm^2 etch would be closer to 37,000 than to the 4,000 monolayers predicted for a constant sputter yield. Since this is a substantial difference in total amount of material removed by IBE at high fluences, it is important to measure the actual removal rate of material as a function of fluence. Such experiments are substantially more difficult to perform, but we are planning to examine this effect and to also analyze other material

systems to ascertain whether or not this is a property unique to graphite or general for other materials.

In summary, the autocovariance function has been used to compress the real space height information from STM and AFM topographs of ion sputtered surfaces to obtain the interface width and correlation length for ion beam eroded surfaces. We found that, for a given flux, both the correlation length and interface width increase with increasing ion beam fluence. For a given fluence, however, the interface widths appear to have a non-monotonic dependence on the ion beam flux, which we do not understand at present. Furthermore, the interface widths at a given flux do not scale with the square root of the fluence, as is expected for a stochastic process. This suggests that the sputter yield of graphite may itself be a function of the fluence, which could result from disruption of the graphite layers that enhances the sputter yield for later IBE. This apparant dependence of the sputter yield on ion beam fluence persists up to fluences of 10^{19} ions/cm^2.

Acknowledgements: This work was supported in part by the Office of Naval Research and by the National Aeronautics and Space Administration.

References

1. *Erosion and Growth of Solids Stimulated by Atom and Ion Beams*, edited by G. Kiriakidis, G. Carter, and J. L. Whitton (Martinus Nijhoff, Hingham, MA, 1986), pp. 70-97.
2. *Ion Bombardment Modification of Surfaces*, edited by O. Auciello and R. Kelly (Elsevier, Amsterdam, 1984).
3. P. K. Hansma and J. Tersoff, J. Appl. Phys., **61**, R1 (1987).
4. R. P. U. Karunasari, R. Bruinsma, and J. Rudnick, Phys. Rev. Lett., **62**, 788 (1989).
5. E. A. Eklund, R. Bruinsma, J. Rudnick and R. S. Williams, Phys. Rev. Lett. 67, 1759 (1991); E. A. Eklund, E. J. Snyder, and R. S. Williams, (to be published).
6. E. A. Eklund, R. S. Williams, and E. J. Snyder, Mat. Res. Soc. Symp. Proc., **157**, 305 (1990).
7. G. Binnig, H. Fuchs, Ch. Gerber, H. Rohrer, E. Stoll, and E. Tosatti, Europhysics Lett., **1**, 31 (1986).
8. M. S. Anderson, Infrared Physics, **31**, 539 (1991).
9. G. Reiss, J. Vancea, H. Wittman, J. Zweck, and H. Hoffman, J. Appl. Phys., **67**, 1156 (1990).
10. D. R. Denley, J. Vac. Sci. Technol., **A 8**, 603 (1990).
11. C. Schœnenberger, S. F. Alvarado, and C. Ortiz, J. Appl. Phys., **66**, 4258 (1989).
12. E. J. van Loenen, D. Dijkkamp, A. J. Hoeven, J. M. Lenssinck, and J. Dieleman, Appl. Phys. Lett., **56**, 1755 (1990).
13. J. F. Ziegler, J. P. Biersack, and U. Littmark,*The Stopping Range of Ions in Solids* (Pergammon Press, New York, 1985).

Figure Captions

Figure 1: Three 2.4μ x 2.4μ atomic force microscope topographs of a graphite surface exposed to a total 5 kev Ar^+ ion fluence of 10^{19} ions/cm^2 at fluxes of (a) $7x10^{13}$, (b) $1.4x10^{14}$, and (c) $7x10^{14}$ ions/cm^2/sec, respectively. All three topographs are plotted so that the x, y and z axes are identically scaled. Note both the asymmetry of feature lengths and the variation of average feature heights.

Figure 2: Plots of the autocovariance as a function (see Eq. 1) of feature separation length for the three topographs shown in Fig. 1. The interface width is the square root of the y-intercept (G(0)) and the average correlation length is the gaussian standard deviation of the autocovariance function at low separation length (R). The dashed curves correspond to the autocovariance parallel to the incoming ion flux projected on the surface; the solid line is the autocovariance perpendicular to the ion flux projection on the surface. At the fluences examined earlier,[5] the two autocovariances did not differ significantly from each other, but at 10^{19} ions/cm^2 the difference is pronounced.

Figure 3: Log-log plot of the interface width δ as a function of the fluence Q for the experimental data presented in Table 1. This plot also shows the predictions of both eqns. 2 and 4; the deviation of the experimental data from a 0.5 power dependence is clearly evident at fluences above 10^{18} ion/cm^2. For the plot of eqn. 4. the best fit parameters Y_0 and β were 1.25 ion/atom and 2×10^{-18} cm^2/ion. respectively.

Table 1: Interface Widths and Correlation Lengths (in Å) as a Function of Sputtering Fluence and Flux.

	Fluence (ions/cm^2)			
	Q_1 (10^{16})	Q_2 (10^{17})	Q_3 (10^{18})	Q_4 (10^{19})
Flux (ions/cm^2/sec)				
J_1 (7×10^{13})				
Interface Width, δ	1.0	3.9	43	258
Correlation Length:				
λ (parallel)[a]	33	135	235	425
λ (perpendicular)[b]	33	135	235	625
J_2 (1.4×10^{14})				
Interface Width, δ	3.3	8.2	92	548
Correlation Length:				
λ (parallel)	40	100	210	1250
λ (perpendicular)	40	100	210	1550
J_3 (7×10^{14})				
Interface Width, δ	20.2	13.1	31.6	448
Correlation Length:				
λ (perpendicular)	20	33	220	525
λ (parallel)	20	33	220	850

[a]Correlation length along the direction parallel to the ion beam incidence.

[b]Correlation length along the direction perpendicular to the ion beam incidence.

Figure 1

(a)

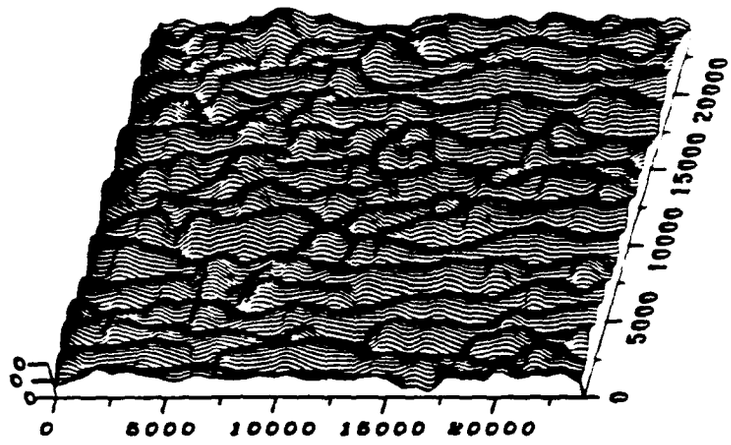
0
5000
10000
15000
20000
0
5000
10000
15000
20000

(b)

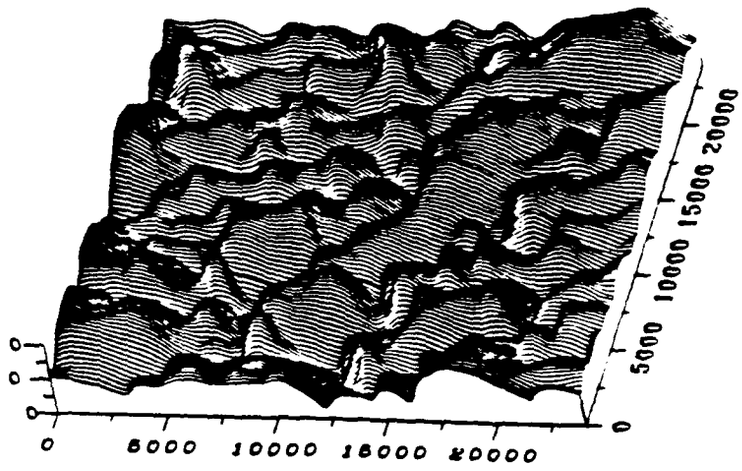
0
5000
10000
15000
20000
0
5000
10000
15000
20000

(c)

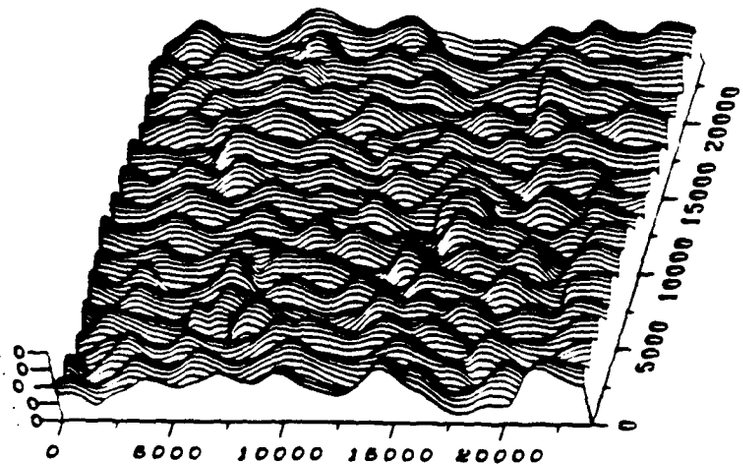
0
5000
10000
15000
20000
0
5000
10000
15000
20000

Figure 2

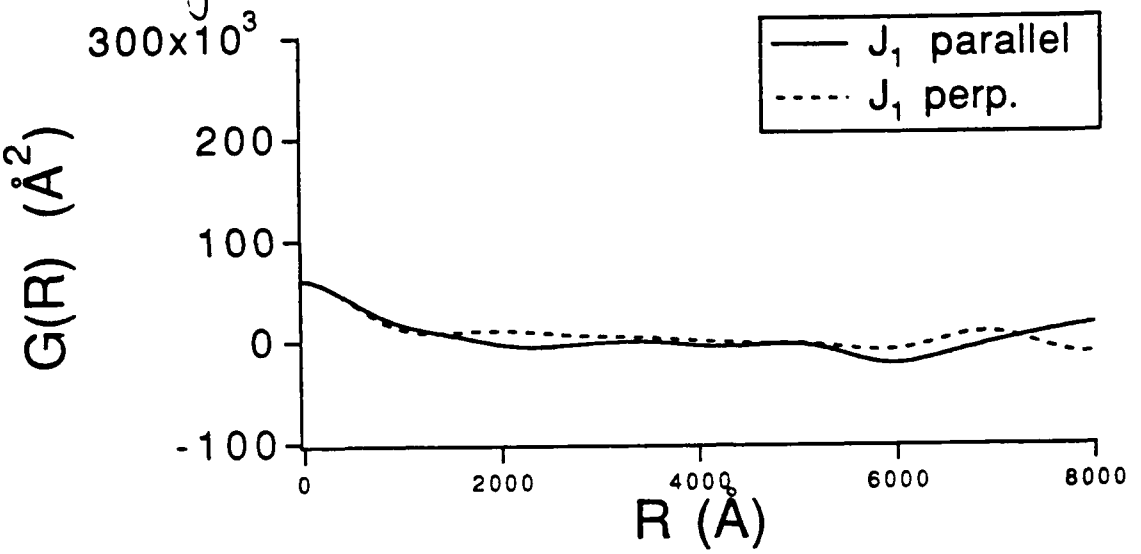
300x10^3
200
100
0
-100
G(R) (Å^2)
0
2000
4000
6000
8000
R (Å)
J1 parallel
J1 perp.

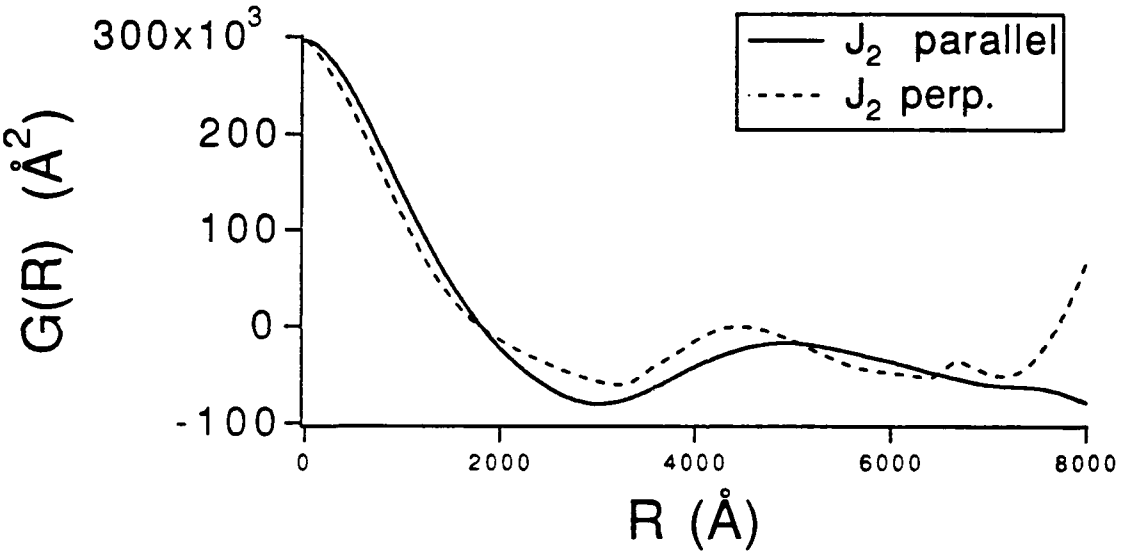
300x10^3
200
100
0
-100
G(R) (Å^2)
0
2000
4000
6000
8000
R (Å)
J2 parallel
J2 perp.

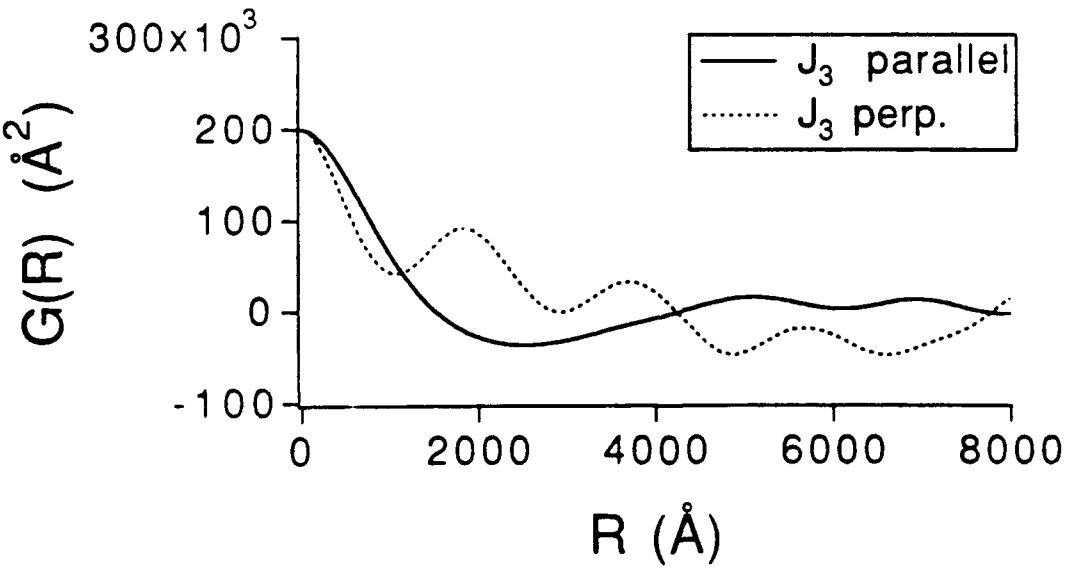
300x10^3
200
100
0
-100
G(R) (Å^2)
0
2000
4000
6000
8000
R (Å)
J3 parallel
J3 perp.

Figure 3

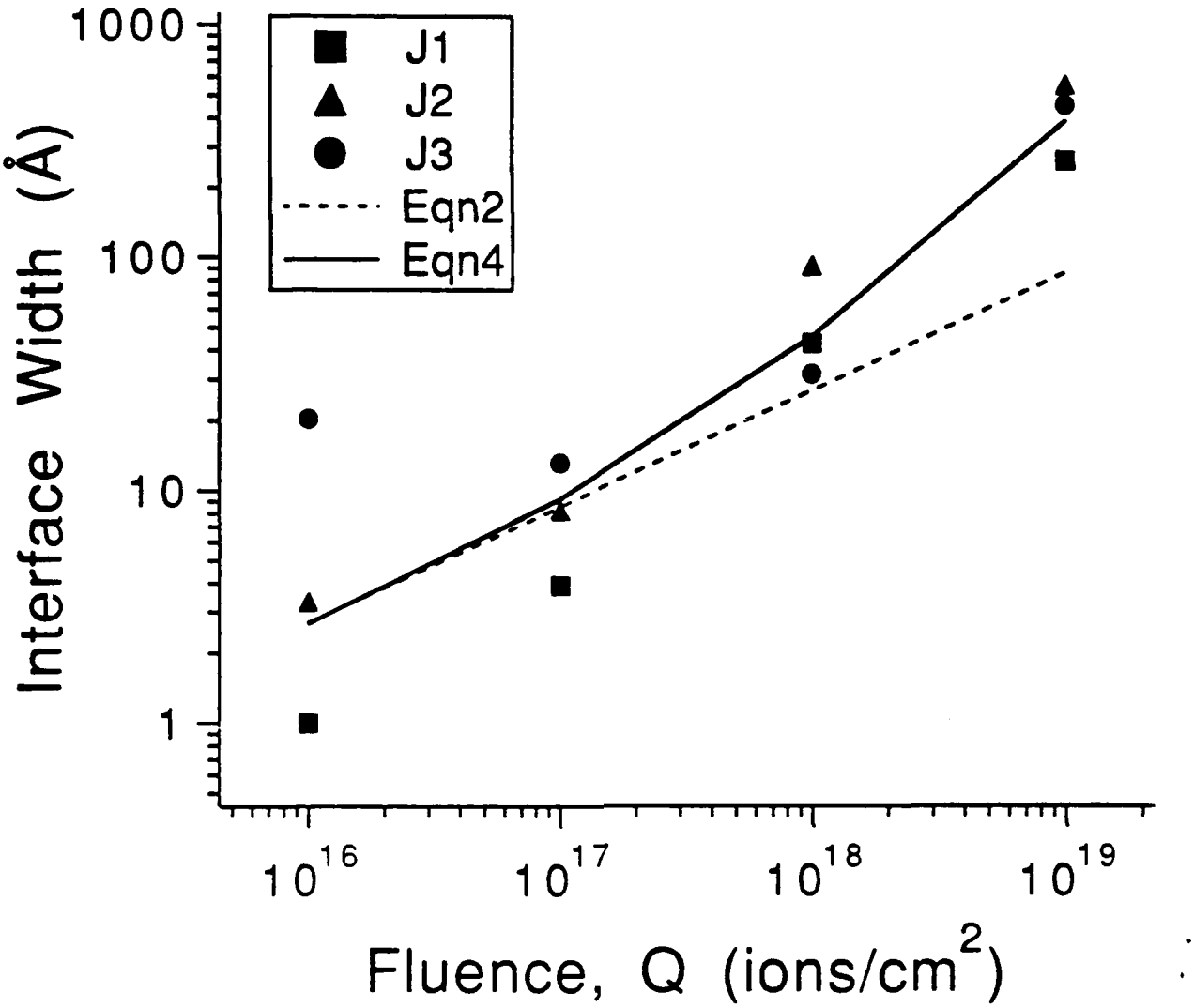
1000
100
10
1
Interface Width (Å)
J1
J2
J3
Eqn2
Eqn4
10^{16}
10^{17}
10^{18}
10^{19}
Fluence, Q (ions/cm^2)